





## Research Article

# Brain Model Based on the Canonical Ensemble with Functional MRI: A Thermodynamic Exploration of the Neural System

Chenxi Zhou <sup>1,2</sup>, Bin Yang <sup>1,2</sup>, Wenliang Fan <sup>3</sup>, and Wei Li <sup>1,2</sup>

<sup>1</sup>School of Artificial Intelligence and Automation, Huazhong University of Science and Technology, Wuhan, Hubei 430074, China

<sup>2</sup>Image Processing and Intelligent Control Key Laboratory of Education Ministry of China, Wuhan, Hubei 430074, China

<sup>3</sup>Department of Radiology, Union Hospital, Tongji Medical College, Huazhong University of Science and Technology, Wuhan, Hubei 430074, China

Correspondence should be addressed to Wei Li; [liwei0828@hust.edu.cn](mailto:liwei0828@hust.edu.cn)

Received 31 March 2021; Revised 16 November 2021; Accepted 17 November 2021; Published 21 December 2021

Academic Editor: Danilo Comminiello

Copyright © 2021 Chenxi Zhou et al. This is an open access article distributed under the Creative Commons Attribution License, which permits unrestricted use, distribution, and reproduction in any medium, provided the original work is properly cited.

**Objective.** System modeling is an important method to study the working mechanisms of the brain. This study attempted to build a model of the brain from the perspective of thermodynamics at the system level, which brought a new perspective to brain modeling. **Approach.** Regarding brain regions as systems, voxels as particles, and intensity of signals as energy of particles, the thermodynamic model of the brain was built based on the canonical ensemble theory. Two pairs of activated regions and two pairs of inactivated brain regions were selected for comparison in this study, and the thermodynamic properties based on the proposed model were analyzed. In addition, the thermodynamic properties were extracted as input features for the detection of Alzheimer's disease. **Main Results.** The experimental results verified the assumption that the brain follows thermodynamic laws. This demonstrated the feasibility and rationality of the proposed brain thermodynamic modeling method, indicating that thermodynamic parameters drawn from our model can be applied to describe the state of the neural system. Meanwhile, the brain thermodynamic model achieved good accuracy in the detection of Alzheimer's disease, suggesting the potential application of thermodynamic models in auxiliary diagnosis. **Significance.** (1) In the previous studies, only some thermodynamic parameters in physics were analogized and applied to brain image analysis, while, in this study, a complete system model of the brain was proposed through the principles of thermodynamics. And, based on the neural system models proposed, thermodynamic parameters were obtained to describe the observation and evolution of the neural system. (2) Based on the proposed thermodynamic models, we found and confirmed that the neural system also follows the laws of thermodynamics: the activation of system always leads to increased internal energy, increased free energy, and decreased entropy as what is discovered in many other systems besides classic thermodynamic system. (3) The detection of neural disease was demonstrated to benefit from the thermodynamic model, which confirmed that the thermodynamic model proposed can indeed describe the evolution of the neural system diseases. And it further implied the immense potential of thermodynamics in auxiliary diagnosis.

## 1. Introduction

The human brain is the most complex organ with unlimited potential. To further understand the physiological principle and working mechanism of the brain, scientists have tried to build models of the brain from different perspectives and then observe and study system states and characteristics. Therefore, dynamics applied in modeling neural systems, called neurodynamics, is an important theory. It attempts to

build neural system models based on dynamics at different levels, from microscopic channels to macroscopic connections of the cerebral cortex. Then, system states and dynamic characteristics can be observed to explore the working mechanism of the brain. Deco and Rolls [1] studied the spiking mechanisms of synapses and neurons under biased competition using dynamic analysis. Based on neurodynamics, Quyen [2] developed, a comprehensive framework to analyze the spatiotemporal characteristics of

the brain on a large scale. Heller and Casey [3] studied the temporal development of adolescents in emotion by building a corresponding model with neurodynamics and explored the relationship between temporal dynamic changes in adolescents with emotional and mood/anxiety disorders. Amari and Maginu [4] built an autocorrelation associative memory model based on statistical neurodynamics to analyze nonequilibrium dynamical behaviors in the recall process. By simplifying the KIII model, Harter and Kozma [5] built a KA model of aperiodic dynamics observed in cortical systems to understand intelligent behavior in biological agents.

The brain network is also significant in modeling neural systems, which are based on function integration and differentiation mechanisms in neurophysiology. The brain network includes the structural brain network and the functional brain network. The structural brain network describes the anatomical links between units, such as the white matter fiber tracts [6]. The functional brain network focuses on describing the interactions between units, for example, the functional correlation [7] or the auto-coherent oscillations of inhibitory neurons [8]. Brain network modeling has also been applied to research on pathologic mechanisms of various neural diseases. Xiang et al. [9] explored the changes in the shortest paths and clustering coefficients of functional brain networks in Alzheimer's disease. Dubbelink et al. [10] studied the changes in brain network topology in Parkinson's disease using magnetoencephalography. Jeong et al. [11] studied the difference in functional brain networks between the epileptic and control groups using global mutual information and global efficiency of different bands with whole-brain magnetoencephalography. The brain network allowed people to diversify out of previous research focusing on one specific independent object, with a view to understand the physiological principle and working mechanism of the neural system at different levels from the perspective of the collaborative working mechanism of the brain.

As mentioned above, the existing works in brain modeling generally focused on the neurodynamics or brain network. While the brain is a multilayered and multidimensional complex system, it is risky to study the brain only from a single level or perspective. In fact, the characterization and understanding of the brain remain inadequate. We still need to try new ways to model and analyze the brain.

Thermodynamics is one of the most important aspects of physics. It focuses on the laws and physical properties of thermal motion and the evolution process of macroscopic matter systems consisting of microscopic particles. Scientists have tried to extend some concepts or theories of thermodynamics into other research fields for general physical state analysis at the system level. In mechanical engineering, Zhang [12] established a theory of nonequilibrium thermodynamics for studying the ThermoPoro mechanical modeling of saturated clays. Albertin et al. [13] used computational thermodynamics to optimize the hardness and wear resistance of high-chromium cast iron. Based on statistical thermodynamics, Kamiyama et al. [14] proposed a "Hakoniwa" method to predict the properties of materials

composed of different types of atoms by calculating the atomic energy. In astronomy, Setare and Sheykhi [15] studied the interaction between viscous dark energy and dark matter in the RSII brane world with thermodynamics. Whitehouse and Bate [16] extended thermodynamics to research the collapse of molecular cloud cores and proposed a three-dimensional algorithm to explore the thermodynamic properties during star formation. In biology, from a statistical thermodynamic point of view, Guo and Brooks [17] proposed a method that made it possible to calculate all thermodynamic properties of a protein model with a specific structure and the free energy surface and compaction processes of the protein model proposed were characterized. Based on the thermodynamics, Fischer et al. [18] generated a distribution of the mixed-canonical ensemble corresponding to different temperatures, and the crossing of energy barriers of RNA was observed by sampling from this distribution. These studies suggest that thermodynamic theory is fundamental and universal to some extent. In other words, its ideas and methods not only allow for research on traditional thermodynamic systems, but are also suitable for system modeling in other fields. Furthermore, thermodynamics can often bring new analytical perspectives for understanding and interpreting systems in other subject areas.

Because of many meaningful results of the researches with thermodynamics applied to those areas, some scientists have tried to evaluate or describe the properties of the brain by defining or using parameters derived from thermodynamics. Zhang et al. [19] used Tsallis entropy from discrete wavelet packet transforming the analysis of brain images and identified glioma, meningioma, and other neural diseases. Wang et al. [20] explored the influence of occupational factors on brain complexity by calculating the brain entropy of seafarers and nonseafarers. Lebedev et al. [21] evaluated the impact of lysergic acid diethylamide on personality using a mixed-effects model based on changes in brain entropy and observed personality during follow-up. Coopting the concept of free energy in informatics, Friston [22] proposed the free energy principle, holding that each biological self-organizing system in equilibrium will minimize the free energy to avoid the "surprise." Friston and Buzsaki [23] attempted to explain the optimization and control mechanisms as well as the functional differentiation of the brain with the proposed free energy principle theoretically. Freeman and Vitiello [24] defined the square of EEG amplitudes as the rate of free energy dissipation to measure the amount of work performed. These studies showed that it is feasible to observe or analyze the brain with specific properties derived from thermodynamics, such as information entropy and free energy in information theory. However, these studies are limited to borrowing concepts from thermodynamics for signal analysis.

Different from the previous studies mentioned above which only defined some parameters learned from the thermodynamic theory to analyze the brain image, this article attempted to construct a thermodynamic model of the brain at the system level based on the canonical ensemble theory. Based on the proposed model, the thermodynamic

parameters were obtained to describe the observation and evolution of the neural system from the perspective of thermodynamics. Through experiments, we verified the rationality and feasibility of the model proposed. The benefit of thermodynamic model towards the detection of neural disease was found, which implied the immense potential of thermodynamics in auxiliary diagnosis. This research tried to explore and characterize the working mechanism of the neural system from a new perspective in order to shed new light on the understanding of the brain.

## 2. Materials and Methods

**2.1. Data Acquisition.** The data used in this study were obtained from Alzheimer’s Disease Neuroimaging Initiative (ADNI) database (<https://adni.loni.usc.edu/>). The ADNI was launched in 2003 as a public-private partnership led by principal investigator Michael W. Weiner, MD. The primary goal of ADNI has been to test whether serial magnetic resonance imaging (MRI), positron emission tomography, other biological markers, and clinical and neuropsychological assessments can be combined to measure the progression of mild cognitive impairment and early Alzheimer’s disease (AD). For up-to-date information, see <https://www.adni-info.org>. One hundred and sixteen patients with AD (age:  $74.6 \pm 7.5$ ) and 174 healthy subjects (age:  $75.5 \pm 6.1$ ) were recruited from ADNI as the AD group and NC (normal control) group, respectively. Demographic information of the subjects is shown in Table 1. There was no significant difference between the two groups in terms of age or sex.

**2.2. Data Preprocessing.** The resting state functional MRI (rs-fMRI) images used in this study were scanned using 3T Philips scanners. The specific operation parameters were as follows: slice thickness, 3.3 mm; number of slices, 48; TR/TE, 3000 ms/30 ms; flip angle,  $80^\circ$ ; and imaging matrix,  $64 \times 64$ . Each series contained 140 volumes. Data preprocessing was performed using SPM8 and DPARSF [25]. The process was as follows: first, the first ten frames were discarded for magnetization equilibrium. Slicing timing and realigning were performed on the time series. Subjects with head rotation exceeding  $2^\circ$  or head translation exceeding 2 mm were excluded. The Montreal Neurological Institute standard human brain template was used to normalize all the corrected image data. Then, the images were smoothed using a  $4 \times 4 \times 4$  Gaussian kernel to decrease spatial noise. The global mean signal was removed to reduce nonneuronal signal fluctuations. The whole brain was divided into 90 regions using an automated anatomical labeling (AAL) template.

**2.3. Denoising with Point Process Method.** The blood oxygen level-dependent (BOLD) signal has been demonstrated to be a description of the hemodynamic response to neural stimulation [26]. Therefore, scientists attempted to search for extreme points of the BOLD signal corresponding to neural stimulation and applied these points to simulate a clear BOLD signal combined with a standard hemodynamic

TABLE 1: Demographic characteristics of subjects.

| Group | Number | Sex (male/female) | Age (year)     |
|-------|--------|-------------------|----------------|
| AD    | 116    | 55/61             | $74.6 \pm 7.5$ |
| NC    | 174    | 97/77             | $75.5 \pm 6.1$ |

equation [27]. Point process analysis holds that there are some significant feature points in the time series of a complex event and the noise can be decreased to highlight the essential nature by extracting these feature points [28]. Therefore, this study used the point process method to remove noise in the BOLD signal for a high signal-to-noise ratio.

The BOLD signal was standardized first. In the time series, the maximum and minimum points were recorded, and the subsequent extreme points were selected as a pair in chronological order. Then, an impulse sequence was obtained by calculating the amplitude increment of every point pair per unit time. Subsequently, we convolved this impulse sequence with the hemodynamic response function proposed by Cohen [29], and a clear BOLD signal was reconstructed.

**2.4. Statistical Thermodynamic Modeling Method.** The canonical ensemble is an important concept in statistical thermodynamics. In statistical thermodynamics, as the system has many different microscopic states under given macroscopic conditions, the measurement of a system is the average of multiple measurements of the system over time. To obtain the measurement at one point, we can measure many identical systems that are under the same macroscopic state at that point and replace the time-average measurement with the average of a large number of identical systems at the same point. The set of a large number of identical systems that are under the same macroscopic state is called an ensemble. Under this premise, the average measurement over time can be replaced by the ensemble average. For an isolated system in equilibrium, in which the energy, volume, and number of particles have all been given, as the probability of possible microscopic states of the system follows the microcanonical distribution, we can analyze the system using the microcanonical ensemble theory. However, it is difficult for most systems to ensure the energy necessary for the microcanonical ensemble analysis. Therefore, researchers generally study a closed system with a given temperature, volume, and number of particles, in which the probability of possible microscopic states of the system follows the canonical distribution. Then, we applied a canonical ensemble to analyze the thermodynamic properties of the system.

Some scientists extended the canonical ensemble or its related theory to the research field of electrochemistry [30], black holes [31–33], biology [18, 34], and so on [35, 36], and the achievements in these fields indicated that the canonical ensemble is universal, but not limited to traditional thermodynamic systems. Thus, we attempted to introduce it to the study of neuroscience. Research has shown that the temperature of the human brain is generally maintained at

36.9 ± 0.4°C [37]. In addition, the volumes and voxels of different brain functional regions are certain for each subject in neuroimaging. If we consider the voxels as particles inside the brain region, the number of particles can be determined. Meanwhile, brain regions do not exchange voxels with the outside; in other words, there is no “matter” exchange in the brain region. Then, the brain region basically meets the requirements of a closed system. Therefore, we believe that the brain region can be regarded as a thermodynamic system whose microscopic states conform to the canonical distribution. Then, we can build a brain thermodynamic model based on the theoretical framework of the canonical ensemble.

Based on the analysis above, this study proposes a brain thermodynamic model. We regarded the brain functional region as a system consisting of nearly independent particles. Each voxel in neuroimaging corresponds to one nearly independent particle. The BOLD signal intensity of fMRI reflects the metabolic intensity, and a higher BOLD signal indicates a higher metabolic level, leading to an increase in oxygen consumption and an increase in energy consumption. Therefore, the energy  $E$  of the voxel was defined as the amplitude of the corresponding reconstructed BOLD signal in this study, and the physiologically activated intensity of each voxel can be evaluated by energy  $E$ . Because the relevant computational data had been standardized, all calculated results were dimensionless.

Each frame of voxel is considered to be a microscopic state of it, and  $Z_i$  is the partition function of the microscopic state of the voxel at the  $i$ -th frame, which can be calculated as

$$Z_i = \exp(-\beta E_i), \quad (1)$$

where  $E_i$  is the energy of the voxel at the  $i$ -th frame and the specific expression of  $\beta$  is as follows:

$$\beta = \frac{1}{kT}, \quad (2)$$

where  $k$  is the Boltzmann constant in thermodynamics, which is equal to 1 to simplify the calculation in this study. The thermodynamic temperature  $T$  is 310 K, which is equal to 37°C, the theoretical temperature of the human brain. The whole brain can represent the environment of brain regions.

If we consider each time point of the BOLD time series to one voxel as a microscopic state, the partition function of the voxel can be calculated by summing all microscopic states, and the computational formula is described as

$$Z_r = \sum_i Z_i = \sum_i \exp(-\beta E_i), \quad (3)$$

where  $Z_r$  is the partition function of the voxel and  $\sum_i Z_i$  is the sum of its microscopic states at all points in the BOLD time series. Owing to the indistinguishability of identical particles and ignoring the weak interactions among particles, we regard a voxel as a subensemble of the brain region. Therefore, the partition function of the brain region is a combination of all voxels inside. The partition function of the brain region,  $Z_{br}$ , can be derived from  $Z_r$ :

$$Z_{br} = \frac{1}{N!} \prod_r Z_r, \quad (4)$$

where  $\prod_r Z_r$  is the quadrature of the partition function of all voxels in the brain region and  $N$  is the number of voxels.

Based on the theoretical framework of the canonical ensemble, we constructed a brain thermodynamic model regarding brain regions as systems, voxels as particles, the intensity of reconstructed BOLD signals as the energy of particles, and the points of fMRI time series as different microscopic states. We referred to this model as the brain thermodynamic model (BrainTDM). This model attempted to describe the working mechanism of the neural system from a thermodynamic point of view.

Based on the BrainTDM proposed in this paper, the internal energy, free energy, and entropy of the neural system can be defined to evaluate the thermodynamic characteristics of brain regions.

The internal energy,  $U$ , of the brain region can be calculated as

$$U = \sum_r U_r = \sum_r \frac{\sum_i [E_i \exp(-E_i/kT)]}{Z_r}. \quad (5)$$

The free energy,  $F$ , of the brain region can be calculated as

$$F = U - TS = -kT \ln Z_{br} = -\frac{kT \log_{10} Z_{br}}{\log_{10} e}, \quad (6)$$

where  $e$  is the Euler number, approximately equal to 2.71828.

The entropy,  $S$ , of the brain region can be calculated as

$$S = k \ln Z_{br} - k\beta \frac{\partial}{\partial \beta} \ln Z_{br},$$

$$U = -\frac{\partial}{\partial \beta} \ln Z_{br}, \quad (7)$$

$$F = -kT \ln Z_{br},$$

$$S = k \ln Z_{br} - k\beta \frac{\partial}{\partial \beta} \ln Z_{br} = -\frac{F}{T} + \frac{U}{T} = \frac{U - F}{T}.$$

For a specific brain region, internal energy represents the statistical average energy of all microscopic states in the system, free energy represents the energy of the brain region that could be used to perform external work, and entropy represents chaos of the brain region after being affected by the external environment. Based on thermodynamics, we supposed that when the brain region was activated and consumed external energy to do work, the energy it contained and the energy to do work would both increase and its internal state could be more orderly compared with inactivated brain regions.

**2.5. Experimental Design.** In this experiment, the fMRI of the brain was processed using SPM8 and divided into 90 brain regions with the AAL template. The point process method was applied to reconstruct clear BOLD signals as

inputs for the following model. In modeling, brain regions were regarded as systems, voxels were regarded as particles, and the intensity of BOLD signals was regarded as the energy of the particles. Then, a brain thermodynamic model was built based on the ensemble theory. The related thermodynamic parameters were calculated, including the partition function  $Z$ , internal energy  $U$ , free energy  $F$ , and entropy  $S$ . More analyses were performed to explore the potential applications of this model.

*2.5.1. Experimental Paradigm I.* In thermal physics, once the thermodynamic system consumes external energy to perform work, the entropy decreases, and the internal energy as well as the free energy increases. We assume that the brain system also follows this rule. That is, when the brain regions are activated with neurons that consume external energy to fire synchronously and sequentially, the thermodynamic parameters of brain regions will change in the same way. In experiment paradigm I, we evaluated the proposed modeling method by analyzing the thermodynamic parameter features of activated and inactivated cerebral regions. Because the default mode network (DMN) is most commonly shown to be activated when a person is not focused on the outside world and the brain is at wakeful rest [38, 39], we selected the medial prefrontal cortex (mPFC), which is a key brain region of the default network as the object of the study. Meanwhile, considering the constant sound stimulation during fMRI scanning, we also selected the Heschl gyrus (HES), which is mainly located in the primary auditory cortex, as the object of the study [40]. Furthermore, we selected the precentral gyrus (PreCG), which is also referred to as the primary motor region or primary motor cortex that belongs to the task-positive network, and the olfactory cortex (OLF), which is a key component of the limbic system, as the controls [39]. The brain regions selected for the analysis are listed in Table 2.

By considering brain regions as systems, voxels as particles, and the intensity of reconstructed BOLD signals as the energy of particles, we constructed the brain thermodynamic models of the selected regions. The thermodynamic parameters of different brain regions were calculated based on the constructed models, including the partition function, internal energy, free energy, and entropy. By analyzing the differences between the thermodynamic parameters of the activated and inactivated brain regions, we attempted to determine whether the neural system also follows the laws of thermodynamics.

*2.5.2. Experimental Paradigm II.* Experiment paradigm II aimed to explore the potential applications of the brain thermodynamic model proposed in computer-aided diagnosis (CAD) or other realistic scenarios. For this purpose, we tried to recognize subjects with AD, taking parameters derived from the brain thermodynamic model as input features. We performed the same classification task with parameters based on the traditional brain network model as a comparison. The specific experiments were performed as follows:

TABLE 2: Selected brain regions. Activated/inactivated indicates that the brain regions were activated/inactivated during fMRI scanning.

| Activated brain regions             | Inactivated brain regions   |
|-------------------------------------|-----------------------------|
| Left/right medial prefrontal cortex | Left/right precentral gyrus |
| Left/right Heschl gyrus             | Left/right olfactory cortex |

- (a) Thermodynamic Parameters—Kendall (TP-Kendall): this experiment constructed the brain thermodynamic model by considering brain regions as systems and voxels as particles. Then, four thermodynamic parameters can be obtained based on this model, namely, the partition function, internal energy, free energy, and entropy. Because 90 brain regions were divided from the cerebral cortex in the AAL template, 360 thermodynamic parameters could be derived as alternative features. According to the cross-validation scheme, 72 parameters with the largest Kendall tau rank correlation coefficients of the training set were chosen and then the same set of features as the test set was used as the input features of the classifiers.
- (b) Thermodynamic Parameters—Expert (TP-Expert): the modeling process of this experiment was the same as that of TP-Kendall, except that we merely chose the thermodynamic parameters from 18 brain regions highly associated with AD based on expertise as features for classification. We also obtained 72 features, as each region had four thermodynamic parameters.
- (c) Brain Network—Kendall (BN-Kendall): this experiment built the functional brain network model traditionally using Pearson’s correlation coefficient to obtain link intensities between 90 brain regions, and 4005 link strengths between brain regions were calculated. Then, according to the cross-validation scheme, 72 link strengths with the largest Kendall tau rank correlation coefficient over the 4005 link strengths of the training set were chosen and the same set of features was used in the test set, which were the input features of the classifiers.

All three experiments selected 72 features for AD detection with the KNN classifier.

### 3. Results

Based on the brain thermodynamic model proposed in this paper, we built models of neural systems in experimental paradigms I and II, and the results are shown. To avoid the influence of accidental factors, a tenfold cross-validation strategy was applied to all classification tasks.

*3.1. Experimental Paradigm I.* Based on the modeling method proposed in this paper, we built a brain thermodynamic model of selected brain regions and obtained the energy of activated and inactivated brain regions for each

subject. In the NC group, we calculated the average energy of each brain region separately and then obtained the corresponding time series trajectory, as shown in Figure 1. The average energy of activated brain regions, mPFC/HES, was significantly higher than that of inactivated brain regions, PreCG/OLF.

Based on the model built, the thermodynamic parameters of each brain region were calculated, including the partition function, internal energy, free energy, and entropy. As the value of the partition function was too large, we took the logarithm in the calculation of this parameter. We calculated the mean of the thermodynamic parameters of different brain regions separately over the NC group, and the results are shown in Figure 2. There were no significant differences between activated brain regions, mPFC, and HES in these thermodynamic parameters. We observed the same phenomenon between inactivated brain regions, PreCG, and OLF. However, there was a significant difference between the activated and inactivated brain regions. The mean values of partition function and entropy in activated brain regions were significantly lower than those in inactivated brain regions, and the internal energy and free energy were the exact opposite.

A  $t$ -test was applied to the thermodynamic parameters of different brain regions, and the results are shown in Tables 3–6. There were significant differences between the activated and inactivated brain regions in all four thermodynamic parameters: partition function, internal energy, free energy, and entropy. There were no significant differences almost in all four thermodynamic parameters among the four activated brain regions; the same result was observed among the four inactivated brain regions.

Furthermore, we attempted to classify brain regions into activated and inactivated regions using thermodynamic parameters as input features with the KNN classifier. Three types of distance measurements were taken in the KNN: correlation distance, cosine distance, and Euclidean distance. The results are presented in Table 7. The classification accuracy fluctuated around 88%, reaching the highest value of 88.66% (cosine distance).

**3.2. Experiment Paradigm II.** In experiment paradigm II, we tried to apply the brain thermodynamic model proposed to the CAD of AD. For comparison, we designed three experiments, namely, TP-Kendall, TP-Expert, and BN-Kendall. These experiments also used KNN as a classifier based on the correlation distance, cosine distance, and Euclidean distance. The results are presented in Table 8. The accuracy of TP-Kendall ranged from 77.14% to 80.47%, with an average of 79.32% and a maximum of 80.47%; the accuracy of TP-Expert ranged from 70.16% to 72.36%, with an average of 71.02% and a maximum of 72.36%, while that of BN-Kendall ranged from 70.51% to 73.28%, with an average of 71.79% and a maximum of 73.28%. Therefore, regardless of whether the Kendall coefficient or expertise was used for feature selection, the recognition accuracies of the proposed brain thermodynamic model were not inferior to those of the brain network model. In particular, with the same feature

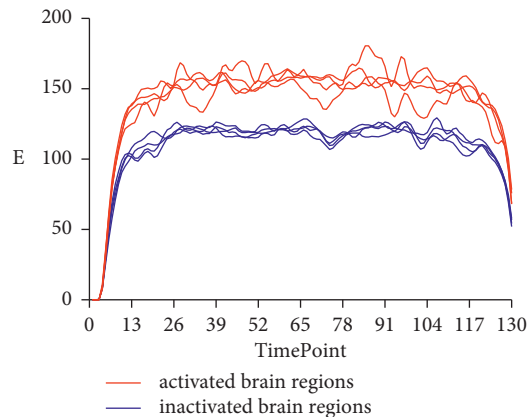


FIGURE 1: Average energy trajectories of activated and inactivated brain regions. The red curves represent the average energy  $E$  of activated brain regions mPFC.L/mPFC.R/HES.L/HES.R, and the blue curves represent the average energy  $E$  of inactivated brain regions PreCG.L/PreCG.R/OLF.L/OLF.R.

selection method, the accuracy of AD recognition based on the thermodynamic model (TP-Kendall) was 7.53% higher than that of the brain network model (BN-Kendall). More specifically, the specificity and sensitivity of TP-Kendall were also 7.60% and 7.43% higher than those of BN-Kendall, respectively, which meant that the thermodynamic model was better for identifying both healthy subjects and patients with AD. In addition, this study focused on thermodynamic modeling, rather than the relationship between specific brain regions and AD, so the brain regions to which the selected thermodynamic parameters belonged would not be discussed.

In this study, both TP-Kendall and BN-Kendall experiments used Kendall for feature selection. Based on these two experiments, we analyzed the impact of different input features on AD recognition using the KNN classifier as described above. The results are presented in Figure 3. Regardless of the number of input features, the accuracy of AD recognition with thermodynamic parameters from the proposed model was always higher than that with link strengths from the brain network model. Furthermore, the accuracy of AD recognition based on the brain thermodynamic model reached 86.34% with only 360 input features in the correlation distance. However, the classification accuracy based on the brain network model peaked only at 85.82% with 4005 input features in the correlation distance.

## 4. Discussion

The brain is the most complex system in the world. Brain modeling is an effective way to explore the work mechanism of the brain and is one of the hottest research topics all the time. Some scientists have attempted to model the brain based on neurodynamic principles and methods, from the microscopic ion channel layer to the macroscopic neural network layer [41]. Most initial studies have focused on the basic working mechanism of neurons or neural connectivity [1, 2, 42]. Later, scientists began to use

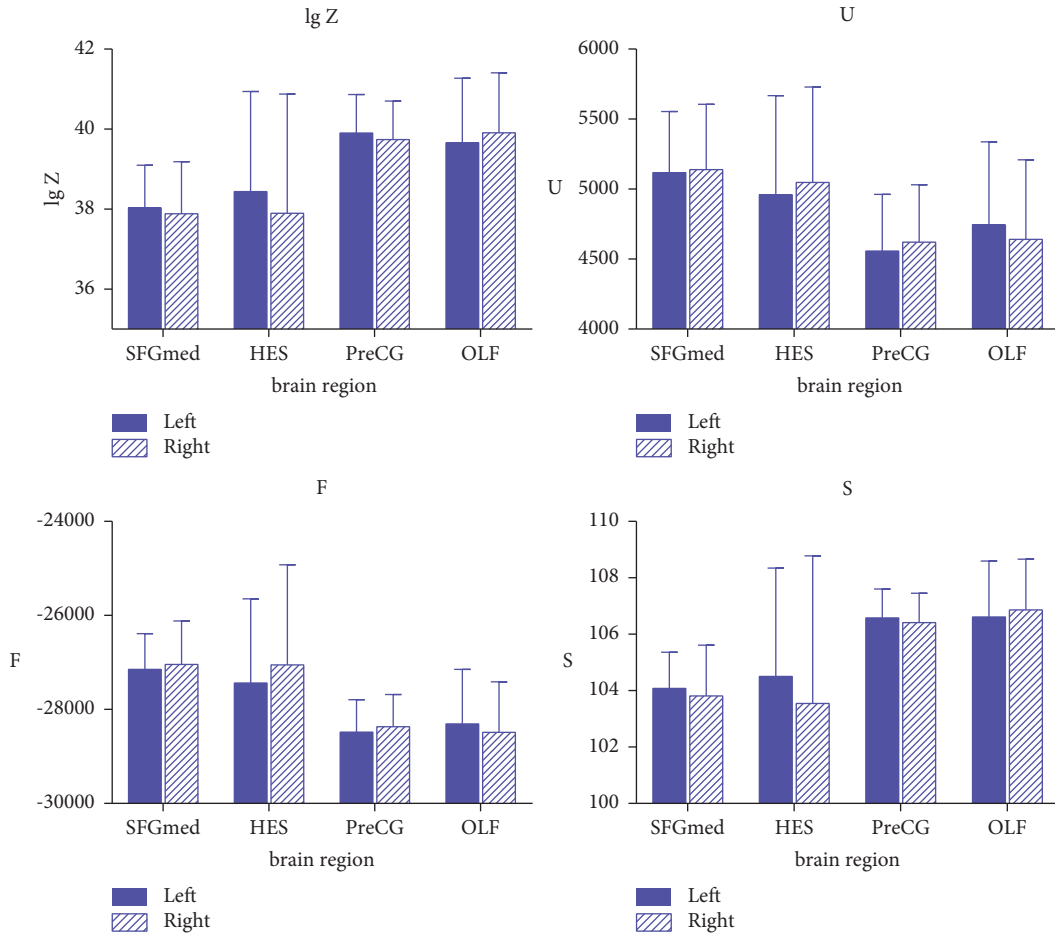


FIGURE 2: Thermodynamic parameters of activated and inactivated brain regions. Left and right represent left brain regions and right brain regions, respectively.

TABLE 3:  $T$  test for  $\lg Z$ .

| Brain region | mPFC.L | mPFC.R | HES.L | HES.R | PreCG.L | PreCG.R | OLF.L | OLF.R |
|--------------|--------|--------|-------|-------|---------|---------|-------|-------|
| mPFC.L       | 1      |        |       |       |         |         |       |       |
| mPFC.R       | 0.25   | 1      |       |       |         |         |       |       |
| HES.L        | 0.05   | 0.01   | 1     |       |         |         |       |       |
| HES.R        | 0.58   | 0.96   | 0.07  | 1     |         |         |       |       |
| PreCG.L      | 0.00   | 0.00   | 0.00  | 0.00  | 1       |         |       |       |
| PreCG.R      | 0.00   | 0.00   | 0.00  | 0.00  | 0.13    | 1       |       |       |
| OLF.L        | 0.00   | 0.00   | 0.00  | 0.00  | 0.09    | 0.54    | 1     |       |
| OLF.R        | 0.00   | 0.00   | 0.00  | 0.00  | 0.96    | 0.22    | 0.13  | 1     |

L and R represent left and right brain regions, respectively.  $P$  value  $< 0.05$  indicates a significant difference.

TABLE 4:  $T$  test for  $U$ .

| Brain region | mPFC.L | mPFC.R | HES.L | HES.R | PreCG.L | PreCG.R | OLF.L | OLF.R |
|--------------|--------|--------|-------|-------|---------|---------|-------|-------|
| mPFC.L       | 1      |        |       |       |         |         |       |       |
| mPFC.R       | 0.67   | 1      |       |       |         |         |       |       |
| HES.L        | 0.01   | 0.01   | 1     |       |         |         |       |       |
| HES.R        | 0.26   | 0.15   | 0.23  | 1     |         |         |       |       |
| PreCG.L      | 0.00   | 0.00   | 0.00  | 0.00  | 1       |         |       |       |
| PreCG.R      | 0.00   | 0.00   | 0.00  | 0.00  | 0.15    | 1       |       |       |
| OLF.L        | 0.00   | 0.00   | 0.00  | 0.00  | 0.00    | 0.03    | 1     |       |
| OLF.R        | 0.00   | 0.00   | 0.00  | 0.00  | 0.12    | 0.70    | 0.10  | 1     |

L and R represent left and right brain regions, respectively.  $P$  value  $< 0.05$  indicates a significant difference.

TABLE 5: *T* test for *F*.

| Brain region | mPFC.L | mPFC.R | HES.L | HES.R | PreCG.L | PreCG.R | OLF.L | OLF.R |
|--------------|--------|--------|-------|-------|---------|---------|-------|-------|
| mPFC.L       | 1      |        |       |       |         |         |       |       |
| mPFC.R       | 0.25   | 1      |       |       |         |         |       |       |
| HES.L        | 0.05   | 0.01   | 1     |       |         |         |       |       |
| HES.R        | 50.58  | 0.96   | 0.07  | 1     |         |         |       |       |
| PreCG.L      | 0.00   | 0.00   | 0.00  | 0.00  | 1       |         |       |       |
| PreCG.R      | 0.00   | 0.00   | 0.00  | 0.00  | 0.13    | 1       |       |       |
| OLF.L        | 0.00   | 0.00   | 0.00  | 0.00  | 0.09    | 0.54    | 1     |       |
| OLF.R        | 0.00   | 0.00   | 0.00  | 0.00  | 0.96    | 0.22    | 0.13  | 1     |

L and R represent left and right brain regions, respectively. *P* value < 0.05 indicates a significant difference.

TABLE 6: *T* test for *S*.

| Brain region | mPFC.L | mPFC.R | HES.L | HES.R | PreCG.L | PreCG.R | OLF.L | OLF.R |
|--------------|--------|--------|-------|-------|---------|---------|-------|-------|
| mPFC.L       | 1      |        |       |       |         |         |       |       |
| mPFC.R       | 0.11   | 1      |       |       |         |         |       |       |
| HES.L        | 0.18   | 0.03   | 1     |       |         |         |       |       |
| HES.R        | 0.19   | 0.53   | 0.05  | 1     |         |         |       |       |
| PreCG.L      | 0.00   | 0.00   | 0.00  | 0.00  | 1       |         |       |       |
| PreCG.R      | 0.00   | 0.00   | 0.00  | 0.00  | 0.15    | 1       |       |       |
| OLF.L        | 0.00   | 0.00   | 0.00  | 0.00  | 0.82    | 0.25    | 1     |       |
| OLF.R        | 0.00   | 0.00   | 0.00  | 0.00  | 0.07    | 0.01    | 0.22  | 1     |

L and R represent left and right brain regions, respectively. *P* value < 0.05 indicates a significant difference.

TABLE 7: Accuracy of classification for activated/inactivated brain regions (%).

| Distance | Correlation  | Cosine       | Euclidean    |
|----------|--------------|--------------|--------------|
| Accuracy | 87.30 ± 0.63 | 88.66 ± 0.64 | 88.57 ± 0.70 |

Correlation, cosine, and Euclidean represent correlation distance, cosine distance, and Euclidean distance.

TABLE 8: Results of the classification for AD/NC (%).

| Feature selection | Distance    | Correlation  | Cosine       | Euclidean    |
|-------------------|-------------|--------------|--------------|--------------|
| TP-Kendall        | Specificity | 84.93 ± 2.21 | 85.18 ± 2.18 | 79.77 ± 2.41 |
|                   | Sensitivity | 73.48 ± 2.45 | 73.41 ± 2.57 | 73.20 ± 2.38 |
|                   | Accuracy    | 80.35 ± 1.71 | 80.47 ± 1.72 | 77.14 ± 1.66 |
| TP-Expert         | Specificity | 73.32 ± 1.30 | 71.81 ± 1.33 | 71.73 ± 1.17 |
|                   | Sensitivity | 70.91 ± 1.91 | 67.69 ± 2.03 | 68.74 ± 1.94 |
|                   | Accuracy    | 72.36 ± 1.00 | 70.16 ± 1.02 | 70.53 ± 1.01 |
| BN-Kendall        | Specificity | 73.55 ± 2.59 | 77.99 ± 2.52 | 75.55 ± 2.60 |
|                   | Sensitivity | 65.96 ± 3.81 | 66.22 ± 3.19 | 65.62 ± 3.58 |
|                   | Accuracy    | 70.51 ± 2.04 | 73.28 ± 1.84 | 71.58 ± 1.95 |

TP-Kendall, TP-Expert, and BN-Kendall represent three different methods of feature selection designed in Section 2.5.2. Correlation, cosine, and Euclidean represent correlation distance, cosine distance, and Euclidean distance.

neurodynamic methods to explain some complicated brain functions, such as emotion, language acquisition, and language comprehension [3, 43, 44], and then developed a method to analyze the pathological mechanisms of epilepsy, AD, and other neural system diseases [45, 46]. In addition, from another perspective, in brain differentiation and integration, scientists have proposed modeling methods for brain networks. Early research has mainly focused on exploring how to construct brain networks from the neuron layer to the functional cortex

layer. The structure equation, causality, correlation, and consistency were applied to the definition of the structure or functional connectivity of the brain [6, 47]. Moreover, scientists have used brain networks to explore the impact of brain lesions on coupling brain regions [48] and the pathological mechanism of neural system diseases, such as brachial plexus injury and AD [49, 50]. Some studies have attempted to extract the characteristics of the brain network for the identification, prediction, and prognosis of diseases and obtained very good results [51–53].



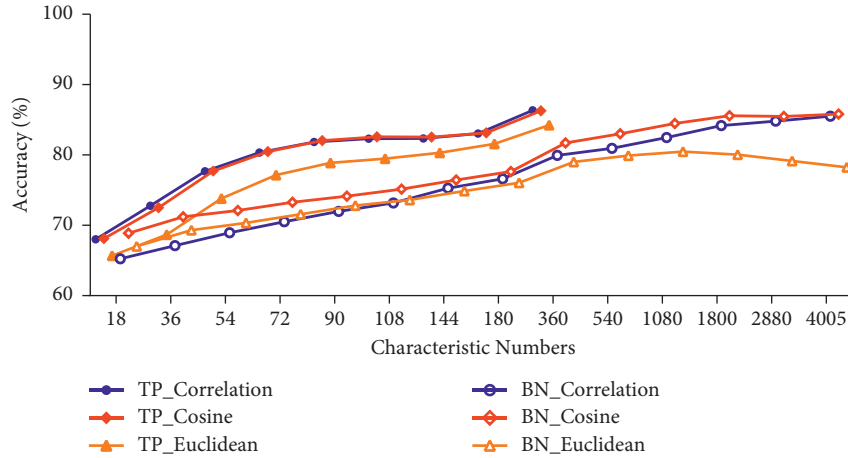


FIGURE 3: Impact of the feature number on accuracy of AD/NC classification.

These modeling methods for the brain have obtained many meaningful results. However, the brain is a typical multidimensional complex system, and the understanding of the brain is inadequate, especially from the point of view of the system.

Thermodynamics, a major branch of physics, mainly studies the thermal properties of an object from the perspective of energy conversion at the macrolevel. Based on the observed phenomenon in the experiment, thermodynamics applies mathematical modeling methods to draw relevant conclusions by logical deduction. Thus, it belongs to phenomenological theory, indicating that the conclusions drawn from this study are highly reliable and universal. Therefore, researchers have always tried to extend and apply related mature theories and concepts of thermodynamics to system modeling and analysis in other research fields, such as mechanical engineering [12–14], astronomy [15, 16], biology [17, 18], economics [54, 55], and other nonclassical physical fields [56–60], in order to realize generalized physical state analysis of objects at the system level in different areas. In this paper, we assumed that the energy conversion of the cerebral cortex is the physical foundation of the brain to implement various complex functionalities. Thus, we assumed that the brain also follows the related macroscopic laws of energy conversion in thermodynamics. When neurons are activated, the brain also consumes the external energy input to work as thermodynamic systems, which leads to increased internal energy, increased free energy, and decreased entropy of the system. Based on the above assumption, we proposed a thermodynamic model of the brain for the first time. Using brain regions as systems, voxels as particles, and the intensity of BOLD signals as the energy of particles, this method built the BrainTDM and tried to explain the work mechanism of the brain based on the canonical ensemble theory from the perspective of energy conversion in thermodynamics.

In experimental paradigm I, we selected two pairs of activated brain regions and two pairs of inactivated brain regions in the resting state as objects. Then, the BrainTDMs of the regions were built and the thermodynamic parameters were calculated. The descriptive statistics and the  $t$  test

results of them were shown in Figure 2 and Tables 3–6, which demonstrated that the internal energy and free energy of activated brain regions (mPFC and HES) were all much higher than those of the inactivated regions (PreCG and OLF), while the opposite was true for the partition function and entropy. This validates the assumption that the brain obeys the laws of thermodynamics at the system level. When activated, the neurons of the specific region burn energy to generate electrical impulses for information transmission, which is doing work just as those thermodynamic systems, leading to the corresponding thermodynamic parameter change of regions: internal energy and free energy increase and entropy decrease. In other words, the brain also follows the laws of energy conversion in thermodynamic systems at the macroscopic level. This was the most important discovery of this study. The results demonstrated that the brain thermodynamic model proposed in this paper is workable and constructing a brain model based on the canonical ensemble theory of thermodynamics is feasible.

We also observed that the energy of activated brain regions was significantly higher than that of inactivated brain regions as shown in Figure 1. This is consistent with the common notion that the activation levels of the mPFC and HES were significantly higher than those of PreCG and OLF in the resting state. For activated regions, the enhancement of DMN activation in the resting state has been demonstrated in many studies, which is consistent with the observation of fMRI imaging in experiments. The activation of the auditory related HES was due to the continuous noise from nuclear magnetic resonance equipment in the experiment. For inactivated regions, PreCG and OLF are related to the control of movement and olfaction, respectively, and were considered to be inactivated due to the resting state. In addition, we tried to classify the brain regions into activated and inactivated regions using the KNN classifier using thermodynamic parameters as input features. The experimental results in Table 7 showed that the classification accuracy remained at approximately 88% and reached the highest 88.66% in three types of distance measurements, correlation distance, cosine distance, and Euclidean distance, which indicated that thermodynamic parameters

could actually reflect the differences in the energy conversion state between activated and inactivated brain regions. In thermodynamics, the internal energy, free energy, entropy, and other thermodynamic parameters are regarded as the common state functions describing the state of the system. This study implied that thermodynamic parameters obtained from the proposed model could also be used as state functions of brain regions to characterize the activated state of brain regions.

Experimental paradigm II attempted to apply the brain thermodynamic model proposed to discriminate diseases of the neural system. With the same feature selection method, the detection of AD based on thermodynamic parameters from the proposed model achieved better results than using link strengths from the traditional brain network model, which was shown in Table 8. According to Figure 3, the accuracy of AD recognition based on the brain thermodynamic model reached 86.34% with only 360 input features. This demonstrated that brain thermodynamic parameters contain some pathological information of neural diseases in nature. This information must be essential and critical in describing the change of brain with diseases, as Figure 3 showed that we could obtain 68.10% accuracy of AD detection with only 18 thermodynamic parameters as input features in cosine distance. The above results indicate that the brain thermodynamic model proposed in this paper not only explains the basic working mechanism of the neural system from thermodynamics, but also has the potential to be applied to the recognition and prediction of neural system diseases. On the other hand, the experimental results also implied that the detection of neural system diseases may benefit from the laws of energy conversion in neural systems.

## 5. Conclusion

In the study of brain modeling, scientists generally focused on neurodynamics or brain network. While brain is a multilayered and multidimensional complex system, we attempted to explore the brain from a new perspective. Drawing on the application of thermodynamics in other fields, we proposed a model of the brain on the system level based on thermodynamics, instead of defining or using some parameters borrowed from thermodynamic parameters. Specifically, this study mapped the neural system to the thermodynamic system by taking brain regions as systems, voxels as particles, and the intensity of BOLD signals as the energy of particles. Based on the canonical ensemble theory, the BrainTDM was built to explore the work mechanism of the brain. The experiment results demonstrated the feasibility and rationality of modeling the neural system from the perspective of thermodynamics, and, on the other hand, they verified the hypothesis that the brain also follows the laws of thermodynamics. In addition, the study also indicated the positive effects of the laws of energy conversion on the detection of neural system diseases, implying that the potential of the model can be applied to auxiliary diagnosis. However, the fMRI only describes the metabolism activities of brain on a macrolevel (brain regions), and we hope that there will be possible validation of the proposed

thermodynamic model from microlevel in the future, such as the microscopic signals (spikes of neuron) from an implantable brain-computer interface. Furthermore, some working mechanisms of the brain may be discovered by combining the thermodynamic properties of macroscopic and microscopic neural signals.

## Data Availability

Data from the ADNI, which was used and analyzed in this study, can be downloaded from the ADNI online repository (<https://adni.loni.usc.edu/>).

## Additional Points

(1) This study applied thermodynamics to the research of neural systems at the system level for the first time. Specifically, thermodynamic models of brain regions were built using extended canonical ensemble theory. (2) The changes in thermodynamic parameters, including higher internal energy, higher free energy, and lower entropy in activated regions, suggested that the neural systems also follow the laws of thermodynamics. (3) The thermodynamic model was proven to benefit from the thermodynamic model through the detection of Alzheimer's disease, which indicates the potential of thermodynamics in auxiliary diagnosis.

## Disclosure

This article has been submitted as a preprint (<https://arxiv.org/abs/2103.01026>) [61].

## Conflicts of Interest

The authors have no conflicts of interest to declare.

## Authors' Contributions

Chenxi Zhou contributed to methodology, software, formal analysis, and writing. Bin Yang contributed to methodology and software. Wenliang Fan contributed to formal analysis and investigation. Wei Li took part in conceptualization, methodology, formal analysis, writing, and funding acquisition.

## Acknowledgments

This work was supported by the National Natural Science Foundation of China (61473131). Data collection and sharing for this project were funded by the Alzheimer's Disease Neuroimaging Initiative (ADNI) National Institutes of Health Grant U01 AG024904) and DOD ADNI (Department of Defense Award number W81XWH-12-2-0012). ADNI is funded by the National Institute on Aging, the National Institute of Biomedical Imaging and Bioengineering, and through generous contributions from the following: AbbVie, Alzheimer's Association; Alzheimer's Drug Discovery Foundation; Araclon Biotech; Bioclinica, Inc.; Biogen; Bristol-Myers Squibb Company; CereSpir, Inc.; Cogstate; Eisai Inc.; Elan Pharmaceuticals,

Inc.; Eli Lilly and Company; EuroImmuno; F. Hoffmann-La Roche Ltd. and its affiliated company Genentech, Inc.; Fujirebio; Healthcare; Ltd.; Janssen Alzheimer Immunotherapy Research & Development, LLC.; Johnson & Johnson Pharmaceutical Research & Development LLC.; Lumosity; Lundbeck; Merck & Co., Inc.; Meso Scale Diagnostics, LLC.; NeuroRx Research; Neurotrack Technologies; Novartis Pharmaceuticals Corporation; Pfizer Inc.; Piramal Imaging; Servier; Takeda Pharmaceutical Company; and Transition Therapeutics. The Canadian Institutes of Health Research is providing funds to support ADNI clinical sites in Canada. Private sector contributions are facilitated by the Foundation for the National Institutes of Health (<https://www.fnih.org>). The grantee organization is the Northern California Institute for Research and Education, and the study was coordinated by Alzheimer's Therapeutic Research Institute at the University of Southern California. ADNI data are disseminated by the Laboratory for Neuro Imaging at the University of Southern California.

## References

- [1] G. Deco and E. T. Rolls, "Neurodynamics of biased competition and cooperation for attention: a model with spiking neurons," *Journal of Neurophysiology*, vol. 94, no. 1, pp. 295–313, 2005.
- [2] M. L. V. Quyen, "Disentangling the dynamic core: a research program for a neurodynamics at the large-scale," *Biological Research*, vol. 36, no. 1, pp. 67–88, 2003.
- [3] A. S. Heller and B. J. Casey, "The neurodynamics of emotion: delineating typical and atypical emotional processes during adolescence," *Developmental Science*, vol. 19, no. 1, pp. 3–18, 2016.
- [4] S.-I. Amari and K. Maginu, "Statistical neurodynamics of associative memory," *Neural Networks*, vol. 1, no. 1, pp. 63–73, 1988.
- [5] D. Harter and R. Kozma, "Chaotic neurodynamics for autonomous agents," *IEEE Transactions on Neural Networks*, vol. 16, no. 3, pp. 565–579, 2005.
- [6] E. Bullmore and O. Sporns, "Complex brain networks: graph theoretical analysis of structural and functional systems," *Nature Reviews Neuroscience*, vol. 10, no. 3, pp. 186–198, 2009.
- [7] J. B. Rowe, "Connectivity analysis is essential to understand neurological disorders," *Frontiers in Systems Neuroscience*, vol. 4, Article ID 00144, 2010.
- [8] S. P. Burns, D. Xing, M. J. Shelley, and R. M. Shapley, "Searching for autocorrelation in the cortical network with a time-frequency analysis of the local field potential," *Journal of Neuroscience*, vol. 30, no. 11, pp. 4033–4047, 2010.
- [9] J. Xiang, H. Guo, R. Cao, H. Liang, and J. Chen, "An abnormal resting-state functional brain network indicates progression towards Alzheimer's disease," *Neural Regeneration Research*, vol. 8, no. 30, pp. 2789–2799, 2013.
- [10] K. T. E. Olde Dubbelink, A. Hillebrand, D. Stoffers et al., "Disrupted brain network topology in Parkinson's disease: a longitudinal magnetoencephalography study," *Brain*, vol. 137, no. 1, pp. 197–207, 2014.
- [11] W. Jeong, S.-H. Jin, M. Kim, J. S. Kim, and C. K. Chung, "Abnormal functional brain network in epilepsy patients with focal cortical dysplasia," *Epilepsy Research*, vol. 108, no. 9, pp. 1618–1626, 2014.
- [12] Z. Zhang, "A thermodynamics-based theory for the thermoporo-mechanical modeling of saturated clay," *International Journal of Plasticity*, vol. 92, pp. 164–185, 2017.
- [13] E. Albertin, F. Beneduce, M. Matsumoto, and I. Teixeira, "Optimizing heat treatment and wear resistance of high chromium cast irons using computational thermodynamics," *Wear*, vol. 271, no. 9–10, pp. 1813–1818, 2011.
- [14] E. Kamiyama, R. Matsutani, R. Suwa, J. Vanhellefont, and K. Sueoka, "The Hakoniwa method, an approach to predict material properties based on statistical thermodynamics and ab initio calculations," *Materials Science in Semiconductor Processing*, vol. 43, pp. 209–213, 2016.
- [15] M. R. Setare and A. Sheykhi, "Thermodynamics OF VISCOUS dark energy IN an RSII Brane world," *International Journal of Modern Physics D*, vol. 19, no. 2, pp. 171–181, 2010.
- [16] S. C. Whitehouse and M. R. Bate, "The thermodynamics of collapsing molecular cloud cores using smoothed particle hydrodynamics with radiative transfer," *Monthly Notices of the Royal Astronomical Society*, vol. 367, no. 1, pp. 32–38, 2006.
- [17] Z. Guo and C. L. Brooks, "Thermodynamics of protein folding: a statistical mechanical study of a small all- $\beta$  protein," *Biopolymers*, vol. 42, no. 7, pp. 745–757, 1997.
- [18] A. Fischer, F. Cordes, and C. Schütte, "Hybrid Monte Carlo with adaptive temperature in mixed-canonical ensemble: efficient conformational analysis of RNA," *Journal of Computational Chemistry*, vol. 19, no. 15, pp. 1689–1697, 1998.
- [19] Y. Zhang, Z. Dong, S. Wang, G. Ji, and J. Yang, "Preclinical diagnosis of magnetic resonance (MR) brain images via discrete wavelet packet transform with Tsallis entropy and generalized eigenvalue proximal support vector machine (GEPSVM)," *Entropy*, vol. 17, no. 4, pp. 1795–1813, 2015.
- [20] N. Wang, H. Wu, M. Xu et al., "Occupational functional plasticity revealed by brain entropy: a resting-state fMRI study of seafarers," *Human Brain Mapping*, vol. 39, no. 7, pp. 2997–3004, 2018.
- [21] A. V. Lebedev, M. Kaelen, M. Lövdén et al., "LSD-induced entropic brain activity predicts subsequent personality change," *Human Brain Mapping*, vol. 37, no. 9, pp. 3203–3213, 2016.
- [22] K. Friston, "The free-energy principle: a unified brain theory?" *Nature Reviews Neuroscience*, vol. 11, no. 2, pp. 127–138, 2010.
- [23] K. Friston and G. Buzsáki, "The functional anatomy of time: what and when in the brain," *Trends in Cognitive Sciences*, vol. 20, no. 7, pp. 500–511, 2016.
- [24] W. Freeman and G. Vitiello, "Nonlinear brain dynamics as macroscopic manifestation of underlying many-body field dynamics," *Physics of Life Reviews*, vol. 3, no. 2, pp. 93–118, 2006.
- [25] C. G. Yan and Y. F. Zang, "DPARSF: a matlab toolbox for "pipeline" data analysis of resting-state fMRI," *Frontiers in Systems Neuroscience*, vol. 4, Article ID 13, 2010.
- [26] S. Ogawa, T.-M. Lee, A. S. Nayak, and P. Glynn, "Oxygenation-sensitive contrast in magnetic resonance image of rodent brain at high magnetic fields," *Magnetic Resonance in Medicine*, vol. 14, no. 1, pp. 68–78, 1990.
- [27] R. L. Buckner, "Event-related fMRI and the hemodynamic response," *Human Brain Mapping*, vol. 6, no. 5–6, pp. 373–377, 1998.
- [28] D. R. Cox and V. Isham, *Point Processes*, CRC Press, Boca Raton, FL, USA, 1980.
- [29] M. S. Cohen, "Parametric analysis of fMRI data using linear systems methods," *NeuroImage*, vol. 6, no. 2, pp. 93–103, 1997.

- [30] M. M. Melander, "Grand canonical ensemble approach to electrochemical thermodynamics, kinetics, and model Hamiltonians," *Current Opinion in Electrochemistry*, vol. 29, Article ID 100749, 2021.
- [31] J. Yang, T. He, and J. Zhang, "Simple harmonic oscillator canonical ensemble model for tunneling radiation of black hole," *Entropy*, vol. 18, no. 11, Article ID 18110415, 2016.
- [32] A. Belhaj and H. El Moumni, "Entanglement entropy and phase portrait of  $f(R)$ -AdS black holes in the grand canonical ensemble," *Nuclear Physics B*, vol. 938, pp. 200–211, 2019.
- [33] Q. Jia, J. X. Lu, and X.-J. Tan, "Phase structures of 4D stringy charged black holes in canonical ensemble," *Nuclear Physics B*, vol. 909, pp. 619–643, 2016.
- [34] M. Poursina and K. S. Anderson, "Canonical ensemble simulation of biopolymers using a coarse-grained articulated generalized divide-and-conquer scheme," *Computer Physics Communications*, vol. 184, no. 3, pp. 652–660, 2013.
- [35] M.-K. Yip, J.-R. Zheng, and H.-F. Cheung, "Persistent current of one-dimensional perfect rings under the canonical ensemble," *Physical Review B*, vol. 53, no. 3, pp. 1006–1009, 1996.
- [36] S. Knani, M. Khalfaoui, M. A. Hachicha, A. Ben Lamine, and M. Mathlouthi, "Modelling of water vapour adsorption on foods products by a statistical physics treatment using the grand canonical ensemble," *Food Chemistry*, vol. 132, no. 4, pp. 1686–1692, 2012.
- [37] H. Wang, B. Wang, K. P. Normoyle et al., "Brain temperature and its fundamental properties: a review for clinical neuroscientists," *Frontiers in Neuroscience*, vol. 8, p. 307, Article ID 00307, 2014.
- [38] M. E. Raichle, A. M. MacLeod, A. Z. Snyder, W. J. Powers, D. A. Gusnard, and G. L. Shulman, "A default mode of brain function," *Proceedings of the National Academy of Sciences*, vol. 98, no. 2, pp. 676–682, 2001.
- [39] D. Zhang and M. E. Raichle, "Disease and the brain's dark energy," *Nature Reviews Neurology*, vol. 6, no. 1, pp. 15–28, 2010.
- [40] P. Morosan, J. Rademacher, A. Schleicher, K. Amunts, T. Schormann, and K. Zilles, "Human primary auditory cortex: cytoarchitectonic subdivisions and mapping into a spatial reference system," *NeuroImage*, vol. 13, no. 4, pp. 684–701, 2001.
- [41] W. Gerstner, W. M. Kistler, R. Naud, and L. Paninski, *Neuronal Dynamics: From Single Neurons to Networks and Models of Cognition*, Cambridge University Press, New York, NY, USA, 2014.
- [42] X. Jiao and R. Wang, "Nonlinear dynamic model and neural coding of neuronal network with the variable coupling strength in the presence of external stimuli," *Applied Physics Letters*, vol. 87, no. 8, Article ID 083901, 2005.
- [43] E. Partanen, A. Leminen, S. de Paoli et al., "Flexible, rapid and automatic neocortical word form acquisition mechanism in children as revealed by neuromagnetic brain response dynamics," *NeuroImage*, vol. 155, pp. 450–459, 2017.
- [44] K. Armeni, R. M. Willems, A. van den Bosch, and J.-M. Schoffelen, "Frequency-specific brain dynamics related to prediction during language comprehension," *NeuroImage*, vol. 198, pp. 283–295, 2019.
- [45] M. L. V. Quyen, V. Navarro, J. Martinerie, M. Baulac, and F. J. Varela, "Toward a neurodynamical understanding of ictogenesis," *Epilepsia*, vol. 44, no. s12, pp. 30–43, 2003.
- [46] J. Jeong, "Nonlinear dynamics of EEG in Alzheimer's disease," *Drug Development Research*, vol. 56, no. 2, pp. 57–66, 2002.
- [47] Y. Yong He, Z. Zhang Chen, G. Gaolang Gong, and A. Evans, "Neuronal networks in Alzheimer's disease," *The Neuroscientist*, vol. 15, no. 4, pp. 333–350, 2009.
- [48] M. Filippi, F. Agosta, E. Scola et al., "Functional network connectivity in the behavioral variant of frontotemporal dementia," *Cortex*, vol. 49, no. 9, pp. 2389–2401, 2013.
- [49] W. W. Wang, Y. C. Lu, W. J. Tang et al., "Small-worldness of brain networks after brachial plexus injury: a resting-state functional magnetic resonance imaging study," *Neural regeneration research*, vol. 13, no. 6, pp. 1061–1065, 2018.
- [50] Z. Yao, Y. Zhang, L. Lin et al., "Abnormal cortical networks in mild cognitive impairment and Alzheimer's disease," *PLoS Computational Biology*, vol. 6, no. 11, Article ID 1001006, 2010.
- [51] C. Y. Wee, P. T. Yap, K. Denny et al., "Resting-state multi-spectrum functional connectivity networks for identification of MCI patients," *PLoS One*, vol. 7, no. 5, Article ID 37828, 2012.
- [52] B. Biao Jie, D. Daoqiang Zhang, W. Wei Gao, Q. Qian Wang, C. Y. Chong-Yaw Wee, and D. Dinggang Shen, "Integration of network topological and connectivity properties for neuroimaging classification," *IEEE Transactions on Biomedical Engineering*, vol. 61, no. 2, pp. 576–589, 2014.
- [53] H. Aerts, M. Schirner, T. Dhollander et al., "Modeling brain dynamics after tumor resection using the Virtual Brain," *NeuroImage*, vol. 213, Article ID 116738, 2020.
- [54] S. A. Rashkovskiy, "Economic thermodynamics," *Physica A*, vol. 582, Article ID 126261, 2021.
- [55] S. A. Rashkovskiy, "Thermodynamics of markets," *Physica A*, vol. 567, Article ID 125699, 2021.
- [56] V. Kocherbitov and I. Argatov, "A thermodynamic theory of sorption in glassy polymers," *Polymer*, vol. 233, Article ID 124195, 2021.
- [57] C. Su, Y. Liu, D. Fan, W. Song, and G. Yang, "Self-consistent thermodynamic parameters of pyrope and almandine at high-temperature and high-pressure conditions: implication on the adiabatic temperature gradient," *Physics of the Earth and Planetary Interiors*, 2021.
- [58] S. Guo, J. Li, B. Zhang et al., "Interfacial thermodynamics-inspired electrolyte strategy to regulate output voltage and energy density of battery chemistry," *Science Bulletin*, 2021.
- [59] A. S. B. de Castro, H. M. C. de Paula, Y. L. Coelho, E. A. Hudson, A. C. S. Pires, and L. H. M. da Silva, "Kinetic and thermodynamic of lactoferrin-ethoxylated-nonionic surfactants supramolecular complex formation," *International Journal of Biological Macromolecules*, vol. 187, pp. 325–331, 2021.
- [60] X. Yang, Z. Mao, X. Zhao et al., "Integrating thermodynamic and enzymatic constraints into genome-scale metabolic models," *Metabolic Engineering*, vol. 67, pp. 133–144, 2021.
- [61] C. Zhou, B. Yang, W. Fan, and W. Li, "Modelling brain based on the canonical ensemble with functional MRI: a thermodynamic exploration of the neural system," 2021, <http://arxiv.org/abs/2103.01026>.